OPTICAL REVIEW Vol. 20, No. 5 (2013) 426–432

Guided Wave Measurements for Characterization of Sol–Gel Layers

Hervé Piombini[1], Xavier Dieudonne[1], Thomas Wood[2], and François Flory[2]

[1]*Commissariat à l'Energie Atomique, DAM LE RIPAULT, F-37260 Monts, France*
[2]*IM2NP, Faculté des Sciences et Techniques, Avenue Escadrille Normandie Niémen, 13397 Marseille Cedex 20, France*

(Received May 15, 2013; Accepted June 19, 2013)

Sol–gel applications require very thick layers with a good understanding of the interfaces. To address this problem, we have installed at CEA Le Ripault a characterization bench using guided waves with assistance from the IM2NP lab in Marseille. This bench allows us to measure the thickness and the refractive index and determine the extinction coefficient of a thin layer. We can distinguish losses at interfaces from those in the bulk according to the chosen propagation mode. This allows us to know if we can stack elementary layers to make thick layers without incurring problems.

Keywords: m-line, sol–gel, refractive index, extinction coefficient

1. Introduction

Sol–gel deposits are well known in the anti-reflective coatings field for having high laser damage thresholds.[1,2] Other applications require very thick layers with a better understanding of the interfaces.[3] Indeed, each porous layer may be built up from several deposition steps. To progress, we must characterize possible interfaces in the monolayers and interfaces between the bilayers. To solve this problem, we have installed at Ripault a characterization bench using guided waves in order to distinguish the surface scattering and bulk scattering, based on the works of the IM2NP lab.[1] This set-up is often used to characterize hard layers manufactured by PVD[5] but rarely to measure layers made by soft chemical processing as the sol–gel method.

2. Measurement Principle

The measurement principle is given in Fig. 1.

The light is injected via a prism in a total reflection configuration,[6,7] in close proximity to a thin film layer. Coupling conditions exist (based on the incidence angle) that allow the light to be guided in this thin film layer. The light is not reflected from the prism base for certain incidence directions and therefore a black line is formed, this black line is called an M-line. The guided light is gradually attenuated along its propagation in the guide by absorption (a) and scattering (s).

If we visualize the light diffused from the thin film layer with a camera, we can quantify this attenuation and determine k the extinction coefficient of the layer $k = k_a + k_s$ with k_a for the thermal part and k_s for scattering part.

3. Guided Waves Theory

The guided waves theory has already been presented several times[4,6] but we prefer here to describe it again in detail. A thin layer of thickness t deposited on a substrate is a planar waveguide if the refractive index of this layer (n_L) is greater than the refractive index of air (n_A) and of the substrate (n_S). That is $n_L > n_S > n_A$.

To inject light into the planar waveguide, we use a prism with a high refractive index.[6,7] We use Maxwell's

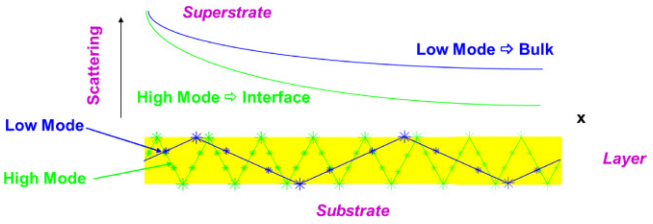

Fig. 1. (Color online) Measurement principle for characterization by guided waves.

equations (1) to find some solutions to this problem:

$$\begin{aligned} \operatorname{rot} \boldsymbol{E} &= \frac{d\boldsymbol{B}}{dt} \quad \boldsymbol{D} = \varepsilon \boldsymbol{E}, \\ \operatorname{rot} \boldsymbol{H} &= \frac{d\boldsymbol{D}}{dt} \quad \boldsymbol{B} = \mu \boldsymbol{H}. \end{aligned} \tag{1}$$

For an electric field which propagates along the z-axis with an E (s) polarization (TE mode), the electric field is written as:

$$E(x, z, t) = E_{0y} \exp[-i(\omega t - k_z z)].$$

The general solution to the electromagnetic wave equation in the three media (n_A, n_L, and n_S) is a linear superposition of waves of the form:

$$E_{0y} \begin{cases} B_A e^{-\alpha_A x} & \text{for } x > t \\ A_L e^{i\alpha_L x} + B_L e^{-i\alpha_L x} & \text{for } 0 < x < t \\ A_S e^{\alpha_S x} & \text{for } x < 0 \end{cases}.$$

We solve Maxwell's equations with the appropriate boundary conditions on this slab waveguide:

$$\begin{cases} \dfrac{k_z}{\omega\mu_0} A_L - \dfrac{k_z}{\omega\mu_0} B_L + \dfrac{k_z}{\omega\mu_0} A_s = 0, \\ -\dfrac{\alpha_L}{\omega\mu_0} A_L + \dfrac{\alpha_L}{\omega\mu_0} B_L - \dfrac{i\alpha_S}{\omega\mu_0} A_s = 0, \\ -\dfrac{k_z}{\omega\mu_0} B_A e^{-\alpha_A t} + \dfrac{k_z}{\omega\mu_0} A_L e^{i\alpha_L t} + \dfrac{k_z}{\omega\mu_0} B_L e^{-i\alpha_L t} = 0, \\ -\dfrac{i\alpha_A}{\omega\mu_0} B_A e^{-\alpha_A t} + \dfrac{\alpha_L}{\omega\mu_0} A_L e^{i\alpha_L t} - \dfrac{\alpha_C}{\omega\mu_0} B_c e^{-i\alpha_L t} = 0. \end{cases}$$

This system has a unique solution if its determinant is zero.

$$-2e^{-\alpha_A t}(\alpha_L(\alpha_A+\alpha_S)\cos\alpha_L t+(\alpha_A\alpha_S+\alpha_L^2)\sin\alpha_L t)=0$$

$$\tan\alpha_L t=\frac{\frac{\alpha_A}{\alpha_L}+\frac{\alpha_S}{\alpha_L}}{1-\frac{\alpha_A\alpha_S}{\alpha_L^2}}$$

$$\Rightarrow \alpha_L t=\arctan\left[\frac{\alpha_A}{\alpha_L}\right]+\arctan\left[\frac{\alpha_S}{\alpha_L}\right]-k\pi.$$

α_A, α_L, and α_S are calculated directly through the Helmholtz's equation (2):

$$\Delta\boldsymbol{E}+k_0^2n^2\boldsymbol{E}=0 \tag{2}$$

with $\Delta\boldsymbol{E}=\Delta E_x\boldsymbol{u}+\Delta E_y\boldsymbol{v}+\Delta E_z\boldsymbol{w}$. A mode will be guided in a thin layer if the propagation constants α_A, α_C, and α_S in the various media satisfy (3):

$$\alpha_L t=\arctan\left[\frac{\alpha_A}{\alpha_L}\right]+\arctan\left[\frac{\alpha_S}{\alpha_L}\right]+m\pi, \tag{3}$$

where t is the thickness of the wave guide. α_A, α_C, and α_S are given by (4):

$$\begin{aligned}\alpha_A^2&=k_z^2-k_0^2n_A^2 \quad \text{in the air,}\\ \alpha_L^2&=k_0^2n_L^2-k_z^2 \quad \text{in the layer,}\\ \alpha_S^2&=k_z^2-k_0^2n_S^2 \quad \text{in the substrate,}\end{aligned} \tag{4}$$

where $k_0=2\pi/\lambda$, $k_z=k\sin\theta$ and λ is the injected wavelength.

This transcendental eq. (3) can be solved graphically with a spreadsheet. For E (p) polarization (TM mode), (5) is the same as (3) except for a scale factor corresponding to $(n_L/n_i)^2$ with $n_i=n_A$ or n_S:

$$\alpha_L t=\arctan\left[\frac{n_L^2}{n_A^2}\frac{\alpha_A}{\alpha_L}\right]+\arctan\left[\frac{n_L^2}{n_S^2}\frac{\alpha_S}{\alpha_L}\right]+m'\pi. \tag{5}$$

4. Determination of Guided Modes

As an example, to determine the guided modes for a 1 µm thickness layer with a refractive index of 1.95 deposited on a silica substrate and coupling with a rutile prism (refractive index 2.87) we can use two methods:

- Either we solve graphically the transcendental eqs. (3) and (5) to obtain θ_L (propagation angle in the layer) by using Excel's solver (see Fig. 2).
- Or we use homemade thin film software and we calculate the reflectance factor versus the incidence angle θ_p (incidence angle in the prism) at a given wavelength (see Fig. 3), in this case at 633 nm.

Both solutions are linked by

$$n_L\sin\theta_L=n_p\sin\theta_p, \tag{6}$$

where the refractive index of the coupling prism is n_p.

For higher order modes, the propagation angle θ_L in the layer is lower and there are more reflections at the interfaces during the wave propagation in the guide. These higher order guided modes will be much more sensitive to interface defects than a propagating wave belonging to a lower order mode, for which the losses are mainly due to bulk scattering.

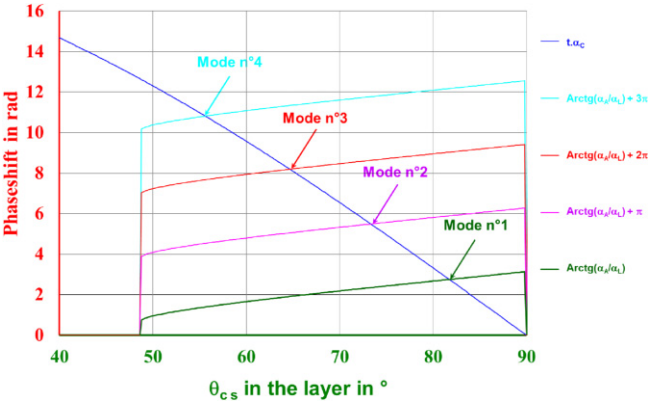

(a)

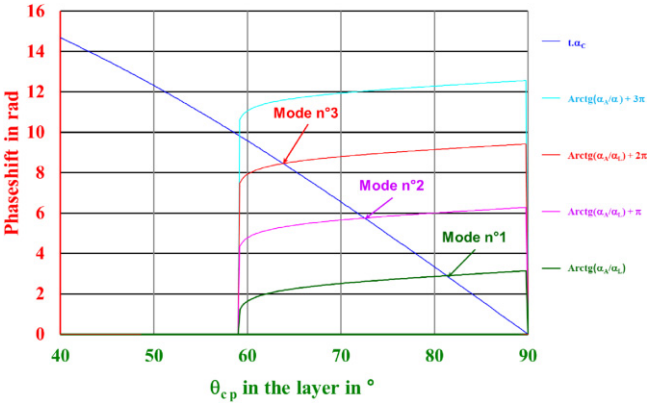

(b)

Fig. 2. (Color online) Solving using transcendental equations for TE mode (a) and TM mode (b).

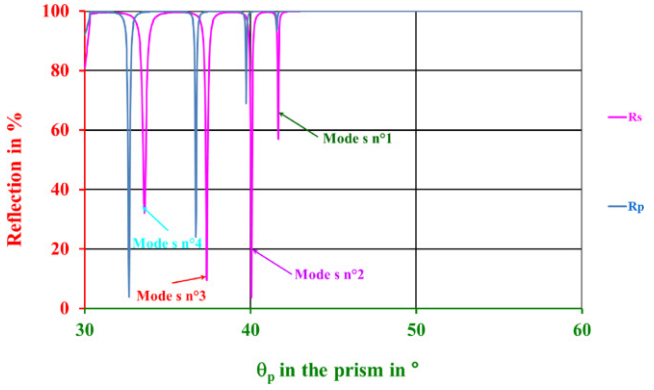

Fig. 3. (Color online) Solving by thin film software.

Therefore by observing the decay of scattered light during the propagation of the guided wave we can try to differentiate between the attenuation effects at interfaces and those induced in the bulk.

5. Experimental Set-up

The experimental set-up and its photograph are given in Figs. 4 and 5. This bench allows us to determine the angles for which light is guided in the thin layer and measure the decay due to scattering of the guided wave.

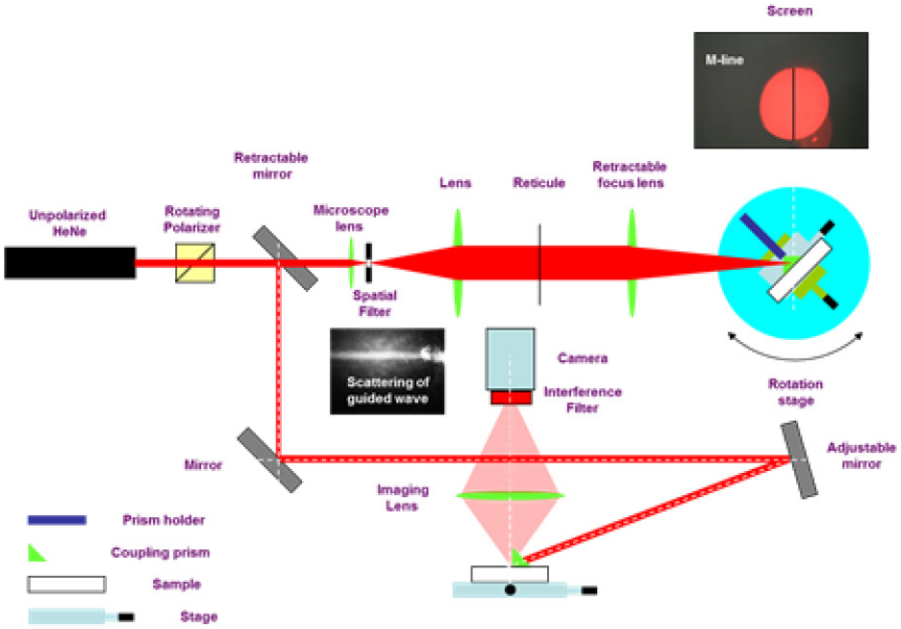

Fig. 4. (Color online) Experimental set-up.

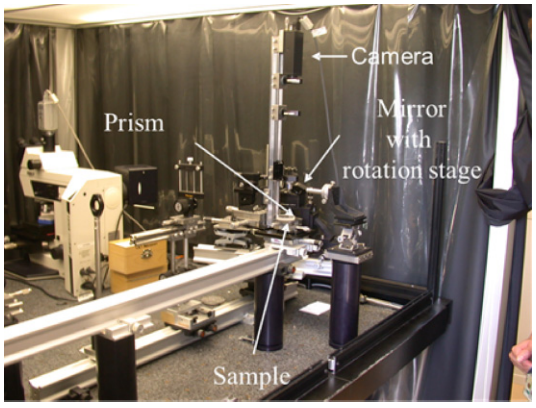

Fig. 5. (Color online) Photograph of experimental set-up.

A HeNe laser is polarized by a Glan prism and injected into a spatial filter by means of a microscope objective. The clean beam is imaged by using two lenses, one of which is retractable, onto the thin layer which is positioned at the center of rotation of a stage. A high index prism of angle A ($A = 45^\circ$ here) made of rutile ($n_e = 2.873, n_o = 2.583$) is fixed on the same rotation stage. This prism is pressed against the layer to minimize the air gap (we note the appearance of equal thickness fringes in white light between the hypotenuse of the prism and the thin layer).[8] The laser beam is focused by the afore-mentioned lenses onto the prism base, hence forming a range of incidence angles, where it is totally reflected. The reflected beam is viewed on a screen and forms a red luminous disc. By rotating the stage, we vary the beam incidence angle on the prism, and for specific angles we couple light into the layer. At these coupling angles, light is not totally reflected and therefore a thin black line appears in the disk of light located on the display screen. The identification of the angular position of this black line (m-line) using a cross hair allows the calculation of the refractive index of the layer if we know its thickness. We have several black lines which appear with the rotation of the stage if the layer is sufficiently thick. With these various modes, we can also calculate the film thickness. The identification of the angle of rotation of the stage θ_m, allows us to evaluate the angle θ_p, which is the angle of incidence at the interface between the prism hypotenuse and the guiding layer [$\sin\theta_m = n_p \sin(\theta_p - A)$], and to calculate the effective refractive index $N_{eff} = n_p \sin\theta_p = n_L \sin\theta_L$. The refractive index of the layer is determined from the effective refractive index the by solving (3) or (5). When multiple coupling angles are available, we put up the retractable mirror to use the second channel of the device to investigate the attenuation of the different modes. We adjust the laser impact onto the intersection of the edge of the prism and tested layer using to x and y linear stages. The layer and the prism are suitably oriented with a θ and ϕ stage and a rotation stage. The impact area is imaged with a lens on a camera. Figures 6 and 7 show the images obtained for impacts where there is a scattering at the edge of the prism for any incidence angle and when a cloud of light exits the prism, indicating that coupling in the thin layer has occurred. An interference filter is added at the camera and a black background level of the sample is removed to increase the image contrast. We must then treat the obtained image, as will be described later.

6. The Investigated Samples

Several samples have been manufactured by PVD and sol–gel methods. The substrates are made of silica or BK7 and have 50 mm diameter and 6 mm thickness. The PVD samples are coated with HfO_2 or ZrO_2 layers deposited by electron beam physical vapour deposition under vacuum with partial pressure of oxygen to obtain layers with a good

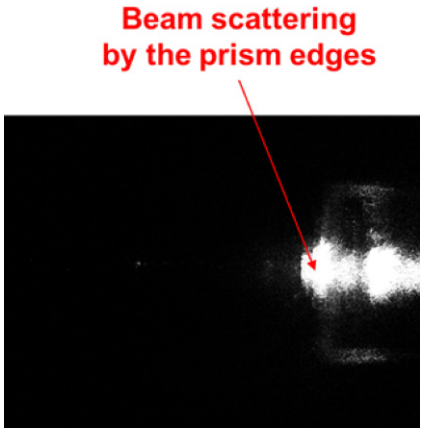

Fig. 6. (Color online) Image when there is not coupling in the layer.

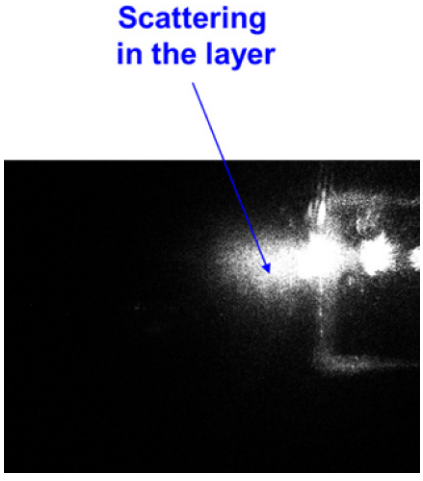

Fig. 7. (Color online) Image when there is coupling in the layer.

stoichiometry. The HfO_2 sample will be our reference sample and will be measured with several methods (ellipsometry, spectrophotometry, and m-lines).

All the sol–gel layers are made of zirconia which is a much researched high index material. For the high index layer, the sol was a colloidal zirconia suspension. It was prepared by urea neutralization of zirconium oxychloride in an aqueous medium followed by hydrothermal crystallization through a method similar to the one described by Somiya et al.[9] The chemical reaction for the synthesis of colloidal zirconia is given by

$$\mathrm{ZrOCl_2 + 2H_2O + H_2N{-}\underset{\underset{\mathrm{O}}{\|}}{\mathrm{C}}{-}NH_2} \xrightarrow[220^{\circ}\mathrm{C}]{20\,\mathrm{bars}} \mathrm{ZrO_2 + CO_2 + 2NH_4Cl.} \quad (7)$$

The crystalline powder was a mixture of monoclinic and tetragonal phases. The aqueous suspension was concentrated under vacuum until it reached 40% oxide by weight, after which, it was diluted by the addition of pure methanol to obtain a mixture with 20% water. To increase the percentage of methanol in the sol, it was necessary to carry out dialysis in methanol. The percentage of methanol was controlled by

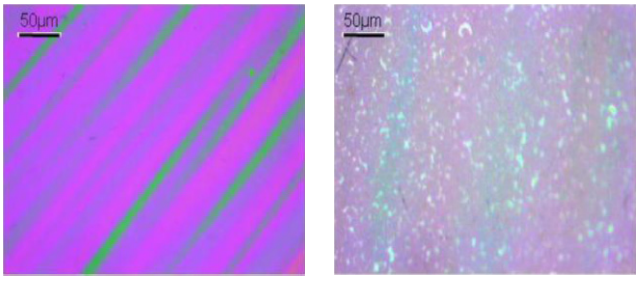

(a) (b)

Fig. 8. (Color online) Example of crack occurrence as verified by optical microscopy for spin-coated silica multilayer stacks. (a) Before crack occurrence and (b) after crack occurrence.

a tensiometry measurement. These sols were then deposited by spin-coating. Preparing thick optical films is known to generate stressed coatings that can lead to crazing, cracking or peeling effects. Indeed, reported limits of the PVD and the sol–gel deposition processes mainly involve the difficulty of achieving thick coatings and to build multilayer stacks.[10–15] The conditions to enabling the increase in thickness of deposited sol–gel films have been studied at the CEA in the past and the determination of these parameters was then correlated to the critical thickness, i.e., the stack thickness before the occurrence of cracks[16] which can be observed by optical microscopy (see Fig. 8).

A stack of ZrO_2 made by sol–gel in methanol solution[9] with several elementary layers of 160 nm thickness has been measured to check its thickness and its refractive index during its processing.

To increase the refractive index of the zirconia layer and the colloidal film cohesion,[17] we add a polymer binder. This polymer is poly(vinyl pyrrodilone) (PVP) which exhibits a good laser damage threshold.[1,2,18] First the PVP is solubilized in a methanol solution then it is added to the colloidal zirconia sol to obtain a nanocomposite sol, with the zirconia accounting for about 17% by weight. The layers named A and C are manufactured with this sol.

7. M-line Results: *n* and *t* Measurements

The PVD sample of HfO_2 was measured with a Varian spectrophotometer in the specular transmission configuration at 0° (Fig. 9) and a Woollam VASE VB-200 Spectroscopic Ellipsometer (Fig. 10) in order to obtain by simulation the thickness and the refractive index of this layer. These values are compared to measurement obtained with our m-line facility.

Table 1 summarizes the results obtained, namely the refractive index n and the thickness t, for the PVD layer of HfO_2.

The obtained results with the m-lines technique are similar to the ellipsometric measurement and near to those from the spectrometric measurement. The PVD sample shows a slight birefringence of the index related to the columnar structure of such deposits.[8] This is neither measured by ellipsometry nor spectrophotometry (our spectrophotometer is not polarized).

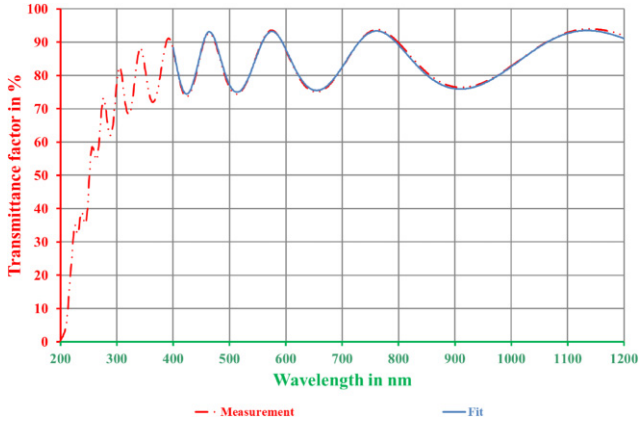

Fig. 9. (Color online) Experimental and fit transmittance factor of the PVD sample.

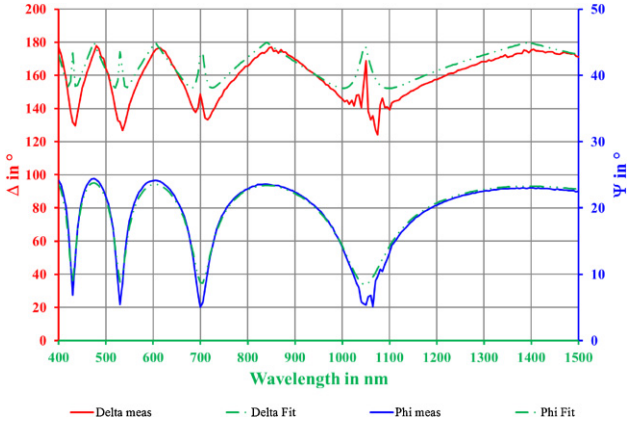

Fig. 10. (Color online) Experimental and fit of Δ and ψ for the PVD sample.

Table 1. Comparison of results obtained with different methods (spectrophotometry, ellipsometry, and m-lines) on the PVD layer.

	θ_m en °		n_{eff}		Results			
	TE(s)	TM(p)	S	P	Refractive index at 633 nm		Thickness (nm)	
					TE	TM	TE	TM
Spectro photometer					2.02		568	
Ellipsometer					1.98		578	
M-lines	TE0: −9.48	TM0: 7.76	1.9117	1.9194	1.959	1.983	589	578
	TE1: −26.23	TM1: −7.57	1.7692	1.7309				
	TE2: −37.81	TM2: −28.19	1.5134	1.4616				

Two sol–gel layers (samples A and C) of PVP poly(vinyl pyrrodilone) zirconia made by spin-coating and two layers of zirconia made by PVD have been measured with the m-lines technique.

A stack of ZrO_2 made by sol–gel in methanol solution[9] with several elementary layers of 160 nm thickness has been measured to check its thickness and its refractive index during its processing. The results are given in Table 3, and show that the refractive index is constant in the stack.

8. Extinction Coefficient Measurement

The absorption measurements presented in Figs. 11 and 12 have been performed for the TE2 mode on layer 2 that has a thickness of 827 nm and for the TE3 mode on layer 3 that has a thickness of 988 nm. Both layers are made of zirconia and deposited by PVD on a BK7 substrate. The incidence angles θ_m of these modes have been determined by m-lines technique (cf. Table 2). We have placed the sample according to θ_m, the determined incidence angle, by moving the sample holder with a camera.

We have recorded the image after subtraction of a background image made without the laser. The best fit line is researched and extracted. We have processed this line with a median filter followed by a decreasing exponential fit:

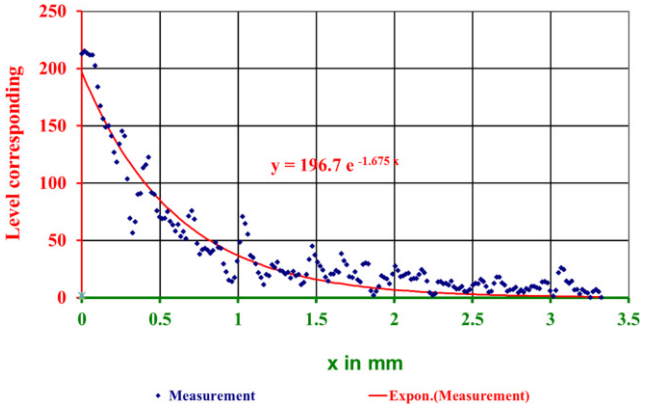

Fig. 11. (Color online) Scattering level of the guided wave for the TE2 mode of layer 2 as a function of distance along its propagation axis.

$N = N_0 e^{-\alpha x}$. The numbers of pixels are translated into the longitudinal dimension with a calibration made by a pattern of known size.

With the knowledge of α and the propagation angle θ_L in the layer, we calculate the extinction coefficient k of the latter ($k = \alpha \sin\theta_L \lambda/4\pi$). Table 4 summarizes the results obtained with the layers of zirconia.

Table 2. Samples and obtained results on various sol–gel and PVD layers.

	θ_m en °		n_{eff}		Results			
	TE(s)	TM(p)	S	P	Refractive index at 633 nm		Thickness (nm)	
					TE	TM	TE	TM
Sol–gel sample A	TE0: −27.814 TE1: −34.196	TM0: −12.243 TM1: −19.137 TM2: −28.250	1.6746 1.5948	1.6703 1.5799 1.4608	1.70	1.699	867	880
Sol–gel sample C	TE0: −32.259	TM0: −16.99	1.6187	1.6081	1.675		530	
PVD sample 2	TE0: 2.32 TE1: −4.2 TE2: −15.08		2.06 1.979 1.839		2.086		827	
PVD sample 3	TE0: −6.55 TE1: −11.22 TE2: −19.22 TE3: −31		1.949 1.889 1.785 1.634		1.971		988	

Table 3. Thickness and refractive index during elementary layer deposition for a ZrO_2 stack.

Numbers of elementary layers	Thickness (nm)	Refractive index (at 633 nm)
3	497	1.693
5	836	1.680
8	1130	1.703
10	1617	1.690

Table 4. Absorption coefficients and extinction layers of zirconia obtained through the use of guided modes.

Layer	n	Mode	α (en m^{-1})	k
2	2.086	TE2	1.675	74×10^{-6}
3	1.971	TE3	1.1196	47×10^{-6}

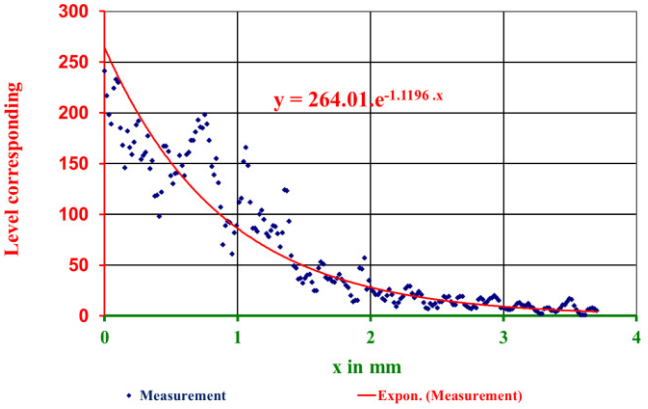

Fig. 12. (Color online) Scattering level of the guided wave for the TE3 mode of layer 3 as a function of distance along its propagation axis.

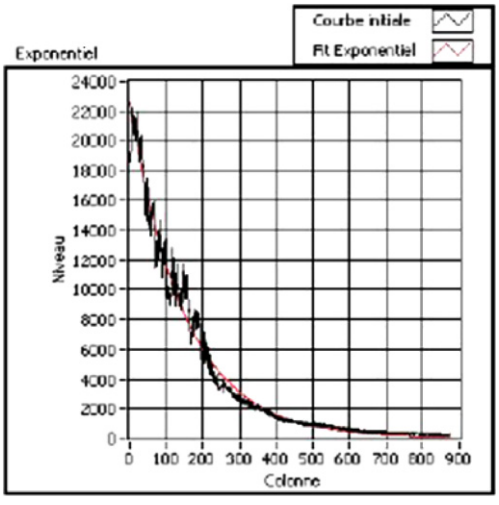

Fig. 13. (Color online) Decay of the recorded scattered light for the ZrO_2 stacks.

For these layers, we have evaluated extinction coefficients close to 10^{-5}, this method being 2–3 orders of magnitude more sensitive than ellipsometric measurements. In a future publication, these measurements will be compared to the mirage effect which measures only the thermal absorption losses in a thin film.[19)]

The Fig. 13 gives a decay signal for a ZrO_2 stack (1617 nm thickness) using the TE2 mode. The attenuation coefficient of this exponential is 0.0066, so the extinction coefficient value k of this stack is equal to 783×10^{-6} ($\theta_L = 72°$).

9. Conclusion

We presented a new characterization bench for thin film layers which gives access to refractive index and thickness measurements. It allows us to measure weak extinction coefficients of thin films that are not accessible by

ellipsometry. This bench, the result of a scientific collaboration between the CEA and the University of Aix-Marseille in Saint Jerome, can also explore the layer interfaces by investigating the influence of interfacial defects on the propagation of high order modes. Bulk effects may be explored from the behavior of low order modes. Due to limitations of our design, particularly high and low order modes are not achievable. With this bench we were able to check that the refractive index of a stack of elementary ZrO_2 layers is constant in the depth of the stack. Soon, the losses measurement will be completely computerized to complement these first results. Then we will compare our measurements with others coming from a similar set-up and those taking into account only the mirage effect.[19)]

References

1) P. Belleville, C. Bonnin, and J.-J. Priotton: J. Sol–Gel Sci. Technol. **19** (2000) 223.
2) Y. Xu, B. Zhang, W. H. Fan, D. Wu, and Y. H. Sun: Thin Solid Films **440** (2003) 180.
3) C. Le Luyer, L. Lou, C. Bovier, J. C. Plenet, J. G. Dumas, and J. Mugnier: Opt. Mater. **18** (2001) 211.
4) F. Flory: in *Thin Films for optical System*, ed. F. Flory (Marcel Dekker, 1995) p. 393.
5) Web [http://www.metricon.com/].
6) R. Ulrich and R. Torge: Appl. Opt. **12** (1973) 2901.
7) S. Monneret, P. Huguet-Chantôme, and F. Flory: J. Opt. A **2** (2000) 188.
8) W. Lukosz and P. Pliska: Opt. Commun. **117** (1995) 1.
9) S. Somaya: in *Advances in Ceramics*, ed. G. L. Messing et al. (Westerville, Ohio, 1987) Hydrothermal Processing of Ultrafine Single-Crystal Zirconia and Hafnia Powders with Homogeneous Dopants.
10) A. E. Ennos: Appl. Opt. **5** (1966) 51.
11) H. Kozuka, S. Takenaka, H. Tokita, T. Hirano, Y. Higashi, and T. Hamatani: J. Sol–Gel Sci. Technol. **26** (2003) 681.
12) H. Kozuka, M. Kajimura, T. Hirano, and K. Katayama: J. Sol–Gel Sci. Technol. **19** (2000) 205.
13) R. Brenier, C. Urlacher, J. Mugnier, and M. Brunel: Thin Solid Films **338** (1999) 136.
14) S. Palmier, J. Neauport, N. Baclet, E. Lavastre, and G. Dupuy: Opt. Express **17** (2009) 20430.
15) A. Mehner, W. Datchary, N. Bleil, H.-W. Zoch, M. J. Klopfstein, and D. A. Lucca: J. Sol–Gel Sci. Technol. **36** (2005) 25.
16) X. Dieudonné, K. Vallé, and P. Belleville: Opt. Express **19** (2011) 16356.
17) A. Ayouch, X. Dieudonné, G. Vaudel, H. Piombini, K. Vallé, V. Gusev, P. Belleville, and P. Ruello: ACS Nano **6** (2012) 10614.
18) L. Zhang, Y. Xu, D. Wu, Y. Sun, X. Jiang, and X. Wei: Opt. Laser Technol. **40** (2008) 282.
19) W. B. Jackson, N. M. Amer, A. C. Boccara, and D. Fournier: Appl. Opt. **20** (1981) 1333.